Improved half-life determination and β-delayed γ-ray spectroscopy for ^{18}Ne decay

G. F. Grinyer, G. C. Ball, H. Bouzomita, S. Ettenauer, P. Finlay, A. B. Garnsworthy, P. E. Garrett, K. L. Green, G. Hackman, J. R. Leslie, C. J. Pearson, E. T. Rand, C. S. Sumithrarachchi, C. E. Svensson, J. C. Thomas, S. Triambak, and S. J. Williams

Phys. Rev. C **87**, 045502 — Published 9 April 2013

DOI: 10.1103/PhysRevC.87.045502

Improved half-life determination and β-delayed γ-ray spectroscopy for ^{18}Ne decay

G.F. Grinyer,[1,*] G.C. Ball,[2] H. Bouzomita,[1] S. Ettenauer,[2] P. Finlay,[3] A.B. Garnsworthy,[2] P.E. Garrett,[4] K.L. Green,[4] G. Hackman,[2] J.R. Leslie,[5] C.J. Pearson,[2] E.T. Rand,[4] C.S. Sumithrarachchi,[4,†] C.E. Svensson,[4] J.C. Thomas,[1] S. Triambak,[2,‡] and S.J. Williams[2,†]

[1] *Grand Accélérateur National d'Ions Lourds (GANIL), CEA/DSM-CNRS/IN2P3, Bvd Henri Becquerel, 14076 Caen, France*
[2] *TRIUMF, 4004 Wesbrook Mall, Vancouver, British Columbia, V6T 2A3, Canada*
[3] *Instituut voor Kern- en Stralingsfysica, K.U.Leuven, Celestijnenlaan 200D, B-3001 Leuven, Belgium*
[4] *Department of Physics, University of Guelph, Guelph, Ontario, N1G 2W1, Canada*
[5] *Department of Physics, Queen's University, Kingston, Ontario, K7L 3N6, Canada*

The half-life of the superallowed Fermi β^+ emitter ^{18}Ne has been determined to $\pm$ 0.07% precision by counting 1042 keV delayed γ rays that follow approximately 8% of all β decays. The deduced half-life, $T_{1/2}$ = 1.6648(11) s, includes a 0.7% correction that accounts for systematic losses associated with rate-dependent detector pulse pile-up that was determined using a recently developed γ-ray photopeak counting technique. This result is a factor of two times more precise than, and in excellent agreement with, a previous lower-statistics measurement that employed the same experimental setup. High-resolution β delayed γ-ray spectroscopy results for the relative γ-ray intensities and β-decay branching ratios to excited states in the daughter ^{18}F are also presented.

PACS numbers: 21.10.Tg, 23.40.Bw, 24.80.+y, 27.20.+n

I. INTRODUCTION

High-precision measurements of the ft values for superallowed Fermi β decays between 0^+ isobaric analogue states provide fundamental tests of the Standard Model description of electroweak interactions. Following the application of small corrections for radiative effects and isospin-symmetry breaking, the resulting $\mathcal{F}t$ values set strict limits on the validity of the conserved-vector-current (CVC) hypothesis, constrain the possibility for the existence of physics beyond the Standard Model, and provide the most precise value for V_{ud}, the up-down element of the Cabibbo-Kobayashi-Maskawa (CKM) quark-mixing matrix [1]. Due to the high precision achieved experimentally, particular attention has recently focused on the theoretical nuclear-structure dependent corrections that account for isospin-symmetry breaking by Coulomb and charge-dependent nuclear forces. In general, these δ_C corrections for the set of the 13 most precise $T = 1$ superallowed emitters range in size from approximately 0.2% for ^{10}C to 1.6% for ^{74}Rb. However, their evaluation depends very sensitively on both the theoretical model employed and the size of the shell-model spaces chosen in the nuclear structure calculations. These model dependencies can be significant with calculated values ranging by factors of four or more depending on the theoretical approach [2–7]. The impact of these model uncertainties on the evaluation of the world-average $\mathcal{F}t$ value and V_{ud} from the set of 13 most precisely measured superallowed decays was recently described in Ref. [8].

Experimental insight into the relative accuracy of these theoretical calculations can be obtained by studying specific decays where the corrections are expected to be large, where nuclear-structure and isospin effects may result in a relative enhancement for a particular case, or where theoretical predictions exhibit the greatest variation [9–15]. The set of $T_z = -1$ superallowed decays are particularly attractive as the isospin-symmetry breaking corrections are, in general, larger than the $T_z = 0$ cases due to the influence of the additional proton that serves to increase the radial-overlap mismatch between the proton and neutron wavefunctions in the parent and daughter nuclei, respectively. However, high-precision measurements of the ft values for these decays are significantly more challenging than for the $T_z = 0$ cases. The parent nuclei are further from stability and production cross sections (beam intensities) are significantly reduced. The daughter nuclei (the $T_z = 0$ emitters) are also unstable and will subsequently β decay giving rise to unwanted but unavoidable time-dependent backgrounds. In addition, several low-lying $T = 0$ states in the daughters can be strongly fed by Gamow-Teller transitions. If the isobaric-analogue state is an excited state in the daughter, determination of the superallowed branching ratio requires a very precise knowledge of the *absolute* γ-ray detection efficiency. This provides a significant experimental challenge that is evidenced by the absence of high-precision ft values for the majority of the $T_z = -1$ emitters. However, given the importance of these particular transitions for potentially discriminating between theoretical corrections of isospin-symmetry breaking, exhaustive detector calibrations using specialized sources and short-lived radioactive beams [16] as well as extensive simulation work have demonstrated that this chal-

*grinyer@ganil.fr
†Present address: National Superconducting Cyclotron Laboratory, Michigan State University, East Lansing, MI 48824, U.S.A.
‡Present address: Department of Physics and Astrophysics, University of Delhi, Delhi 100 007, India

lenge can, to a large extent, be overcome. A branching-ratio measurement performed for ^{22}Mg achieved an overall precision of ± 0.15% [17] and additional cases such as ^{18}Ne, ^{26}Si, ^{34}Ar, and ^{38}Ca will also be feasible in the near future using similar techniques [18].

In the present work, we focus on the $T_z = -1$ superallowed decay of ^{18}Ne to its isobaric analogue, a 0^+ excited state located 1042 keV above the 1^+ ground state in the daughter ^{18}F. The decay level scheme is shown in Fig. 1. This decay is of particular interest for investigating theoretical descriptions of isospin-symmetry breaking as model predictions exhibit some of the largest differences than for any of the other cases. Calculated δ_C corrections range from 0.27%, obtained using a self-consistent relativistic Hartree and Hartree-Fock approach based on the random-phase approximation [4], to 1.41% that was recently calculated using isospin and angular-momentum projected nuclear density functional theory (DFT) [6, 7]. The present standard in this field are the set of shell-model calculations performed by Towner and Hardy whose radial wavefunctions are calculated using a Woods-Saxon mean-field parameterization constrained to experimental binding energies and nuclear charge radii. These calculations yield an intermediate value of 0.57% [2]. The same set of calculations were repeated using Hartree-Fock wavefunctions with different Skyrme interactions and yielded 0.36% [1].

One reason for the large variation in the calculated δ_C corrections for this particular case arises from shape differences between the ^{18}Ne parent and the ^{18}F daughter. Several low-lying intruder states are known in ^{18}F including a deformed 0^- state at 1081 keV that is only 39 keV above the 0^+ analogue state of interest here. In addition, the second 0^+ excited state at 4.75 MeV is located only 3.71 MeV above the 0^+_1 state. Configuration mixing between the spherical 2-particle 0^+ state and the 4 particle, 2-hole 0^+ intruder is enhanced by the relatively small energy difference between these states. The precise degree of mixing between these configurations is difficult to obtain with the shell model and calculations relying on effective interactions [19] while shape differences between the spherical parent and deformed daughter nuclei are known to increase the size of the δ_C corrections obtained with the DFT approach [6, 7].

The ft value for the superallowed decay of ^{18}Ne, $ft = 2919(79)$ s [1], is not yet sufficiently precise to be included in the survey of the 13 highest precision cases. The ft value characterizes any β decay transition and is obtained experimentally from three quantities. The Q value, which is required to calculate the phase-space integral f, has been established to ± 0.02% precision through a ^{18}Ne mass measurement that employed a Penning-trap mass spectrometer [20] in addition to the several concordant measurements of the mass of the daughter ^{18}F and the 1042 keV excitation energy of the 0^+ analogue state [21, 22]. The half-life of ^{18}Ne, $T_{1/2} = 1.6656(19)$ s, was previously determined by our group to ± 0.11% precision [23] from an experiment that

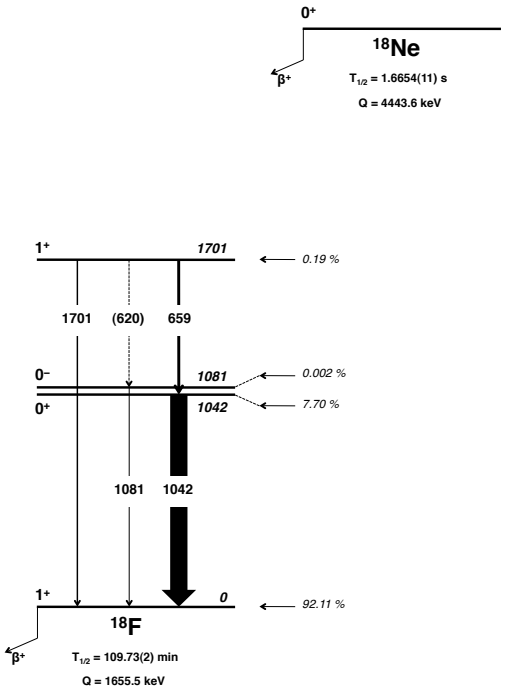

FIG. 1: Decay level scheme of ^{18}Ne.

used the first online beams from a prototype electron-cyclotron-resonance (ECR) ion source developed at TRIUMF's Isotope Separator and Accelerator (ISAC) facility. The absolute branching-ratio to the 0^+ analogue state, $BR = 7.70(21)\%$, was last measured nearly 40 years ago [24] and is currently, by far, the limiting factor in extracting a precision ft value for this decay.

In anticipation of a high-precision branching-ratio measurement, the present study aims to improve upon the previously reported half-life measurement and reduce its overall uncertainty by a factor of two to a level that will be negligible when compared to the expected precision of ∼0.2% that is likely to be achieved in a future measurement of the branching ratio. The half-life measurement follows our previous work [23, 25] and relies on a novel technique that was developed to correct γ-ray gated decay activity curves for rate-dependent detector pulse pile-up effects. Several long implantation activity curves were also measured over the course of the present experiment that have permitted high-statistics measurements of the relative branching ratios and γ-ray yields for various excited states in ^{18}F populated in the β decay. The present article begins with a description of the experimental setup, describes the high-resolution β delayed γ-ray spectroscopy analysis, which was also valuable for assessing the beam purity, and concludes with the improved high-precision half-life measurement for ^{18}Ne.

II. EXPERIMENT

The experiment was performed at the TRIUMF-ISAC radioactive ion-beam facility located in Vancouver, Canada. Radioactive beams of ^{18}Ne were produced from spallation reactions on a thick SiC target induced by a beam of 500-MeV protons, with an average intensity of 70 μA, delivered by TRIUMF's main cyclotron. Reaction products released from the target were subsequently ionized in a Forced Electron Beam-Induced Arc-Discharge (FEBIAD) ion source coupled directly to the target [26]. Singly-ionized, low-energy beams were extracted from the ion source at 60 keV, mass analysed through a $\Delta m/m \approx 1/1000$ mass separator, and sent to the experimental hall. In the present experiment, the beam intensity of ^{18}Ne varied between 8×10^5 ions/s and 2×10^6 ions/s. This was between 2 to 5 times higher than our previous experiment [23] and is primarily due to the higher proton current used on target in the present study (only 30 μA were used previously). A long-lived beam contaminant of ^{18}F ($T_{1/2}$ = 109.7 min [27]) was also present in the mass-separated $A = 18$ beam with an average intensity of 2.5×10^7 ions/s. Analysis of the β-coincident and γ-ray singles spectra (Fig. 2) and the time-dependent γ-ray gated activity curves (Fig. 3) did not provide any evidence for the presence of additional contaminants in statistically significant quantities. A summary of the beam intensities and purities that were delivered in both experiments are compared in Table I.

TABLE I: Comparison between $A = 18$ mass-separated beam intensities I for singly ionized ^{18}Ne, ^{18}F, and ^{17}F isotopes from two separate experiments that used a FEBIAD (F) ion source (present work) and an ECR (E) ion source (Ref. [23]). No evidence for ^{17}F molecular contamination was observed from the FEBIAD source. Values represent upper limits at 90% confidence.

Isotope Species	I_E (ions/s)	I_F (ions/s)	Ratio (F/E)
^{18}Ne	4.0×10^5	8.5×10^5	2.1
^{18}F	1.5×10^6	2.5×10^7	16.3
^{17}F	2.1×10^4	$<3.8\times10^3$	<0.2

Low-energy (60 keV) beams of ^{18}Ne were implanted under vacuum into a moveable mylar-backed aluminum tape at the mutual center of the Scintillating Electron-Positron Tagging Array (SCEPTAR) [28] and the 8π γ-ray spectrometer [29, 30]. The 8π is a spherical array consisting of 20 coaxial high-purity germanium (HPGe) detectors and covers $\sim$13% of the 4π solid angle. The absolute photopeak efficiency of the array is approximately 1.0% for 1.3 MeV photons. The back and sides of each HPGe crystal are surrounded by bismuth-germanate (BGO) scintillators that can be used for Compton suppression and their front faces are collimated with 2.54 cm thick heavy metal (tungsten alloy) that prevents γ-rays from directly striking the BGO. The collimators are covered with 1 cm thick plastic (delrin) absorbers that are used to minimize the amount of bremsstrahlung radiation produced from energetic β particles from reaching the detectors.

Preamplifier output signals from the HPGe detectors were split into two branches for energy and timing purposes, respectively. The energy signals were amplified using Ortec 572 spectrosocopy amplifiers and shaping times were varied between 0.5, 1.0, and 2.0 μs throughout both experiments. Analogue output signals were then digitized using Ortec AD114 14-bit peak-sensing analogue-to-digital convertors (ADCs). The inhibit output signals, generated from an internal pile-up rejection circuit incorporated in the amplifiers, were used in the subsequent analysis for performing detector pulse pile-up corrections. An adjustable front-panel potentiometer was used to manually set the threshold of the gated baseline restore as close as possible to the noise level. The second set of HPGe preamplifier outputs were sent to a timing-filter amplifier and were discriminated using Ortec 583b constant-fraction discriminators (CFDs). The fast outputs of the CFDs were used to generate both the trigger logic and the HPGe timing relative to the delayed master trigger using 32-channel LeCroy 3377 multi-hit time-to-digital convertors (TDCs) operated in common-stop mode. Additional TDC modules were used for the 20 BGO timing signals for optional Compton suppression to be performed in software (not used in the present analysis since the rate-dependent probability of false vetos are known to bias the resulting half-life determination [25]) and for the 20 pile-up detection inhibit signals from the spectroscopy amplifiers for performing the pile-up corrections. If one or more hits were recorded in the pile-up TDC of a particular detector and if there was a corresponding time in the germanium TDC for that same detector, the event was considered to be piled up. Analysis of the time-dependent ratios of piled-up events to the total number of trigger events were then used to quantify and apply the pile-up corrections to the γ-ray gated decay data according the method described in Ref. [25].

The 20 plastic (BC-404) scintillators of SCEPTAR each have a thickness of 1.6 mm and were arranged into four pentagonal rings so that one plastic was positioned directly in front of each of the 20 HPGe detectors. The detectors were mounted inside a spherical plastic (delrin) implantation chamber that housed the moving tape and surrounded the beam implantation site. The entire ensemble was under vacuum during beam delivery. Each scintillator was positioned approximately 3 cm from the beam collection point. The solid angle coverage of the entire array was $\sim$80%. The 20 scintillators were optically coupled to plastic (lucite) light guides that were used to transport the scintillation light to photomultiplier tubes located outside the array. Signals from the photomultiplier tubes were amplified with Phillips 776 fast amplifiers. One of the outputs of the fast amplifiers were delayed and digitized using 12-bit LeCroy 4300 fast-encoding readout amplifier (FERA) charge-

to-digital convertors (QDC). The second outputs were discriminated using Ortec 935 CFDs and were sent to LeCroy 3377 TDCs for timing. Additional signals from the CFDs were used to generate the trigger logic and were multi-scaled using a 32-channel scalar in VME.

Event-by-event β- and γ-ray trigger data generated from the SCEPTAR and the 8π data streams were individually time stamped to 100 ns precision using two LeCroy 2367 Universal Logic Modules. The time standard for the data acquisition was a 10 MHz $\pm$ 0.1 Hz dual-ovenized oscillator from Stanford Research Systems. The trigger was selected in software between singles events from one or both streams (with a rate divided option), and/or hardware coincidences between the two. Using the event-by-event time-stamp information, β-γ coincidences were reconstructed in the offline analysis. Dead times of the data acquisition were also determined on an event-by-event basis using the time-stamp information. Their values could also be specified and fixed for a non-extendible duration for every trigger event. In both experiments, dead-times were periodically varied on a run-by-run basis between a "variable" setting (measured event-by-event) and fixed and non-extendible durations of either 27 μs or 40 μs, which were both chosen to be larger than the maximum time required by the data acquisition for processing any single event.

A. Delayed γ-ray spectroscopy

Data were collected in cycles that consisted of a period of background counting t_b, a beam-on-tape collection period of t_c, and a beam-off (decay) measurement interval of duration t_d. The tape was then moved a distance of 1.5 m to remove any residual and daughter activities from the collection and counting position to a shielded tape storage box outside the array. All cycling times and tape movements were controlled by the data acquisition with a Jorway 221 timing and sequence module. Implantation and decay cycles with a total duration of t_b+t_c+t_d were optimized depending on the particular beam of interest, the half-life of its decay, and those of the contaminants and daughters (if present). The moving-tape collector system was necessary in the present study to remove the long-lived ^{18}F activity that was delivered in the beam itself and was produced as the daughter of ^{18}Ne decay.

Several long cycles, each with a total duration of 171 s, were recorded to search for and quantify potential beam contaminants in addition to the known ^{18}F daughter activity. All of these cycles had a time structure of 10-120-40-1 s corresponding to t_b, t_c, t_d, and the tape movement, respectively. The trigger for the data acquisition, which was running continuously throughout each cycle, was generated from β-γ coincidence events, or γ-ray singles events detected in the 8π spectrometer, or β singles events detected in SCEPTAR with a scale-down factor of 100 applied. The maximum instantaneous rates that were observed in SCEPTAR and the 8π spectrometer were 6×10^5 Hz and 3×10^4 Hz, respectively.

TABLE II: Relative γ-ray intensities (I) deduced in the present work and comparison to previous results.

E_γ (keV)	I_γ/I_{1042} (%)	Ref. [24] (%)	Ref. [32] (%)	Ref. [33] (%)
620	$<0.003^a$	—	—	—
659	1.733(12)	2.1(3)	1.69(4)	1.72(5)
1042	100	100	100	100
1081	0.0288(27)	—	0.0297(22)	0.0289(26)
1701	0.659(7)	0.71(17)	0.646(21)	0.687(13)

[a]Upper limit with 90% confidence. See text for details.

TABLE III: Relative β-decay branching ratios (B) deduced in the present work and comparison to previous results.

E_{level} (keV)	I^π	B/B_{1042} (%)	Ref. [24] (%)	Ref. [32] (%)	Ref. [33] (%)
1042	0^+	100	100	100	100
1081	0^-	0.0278(31)	—	0.0278(33)	0.0270(35)
1701	1^+	2.436(14)	2.87(35)	2.376(46)	2.449(53)

Singles and β-coincident γ-ray spectra are presented in Fig. 2(a) for all data collected in the second experiment with amplifier shaping times of 2 μs. These spectra include the data that were obtained with the shorter cycling times optimized for the half-life measurement described below in Sec. III. A time gate has been applied to select only those γ rays collected between the start of the beam-on period and up to 15 s ($\sim$9 half-lives of ^{18}Ne) after the beam was turned off. All delayed γ rays observed to follow ^{18}Ne decay: 659 keV, 1042 keV, 1081 keV, and 1701 keV, are known from previous studies [31–33]. All other γ-ray transitions observed in Fig. 2(a) originate from summing effects, are single- or double-escape events from higher-energy γ rays, or are known room background. In Fig. 2(b), the 1081 keV γ-ray that follows the weakly fed first-forbidden $0^+ \rightarrow 0^-$ β-decay branch is highlighted. This transition has been studied previously to quantify pion-exchange contributions to the nuclear axial current and to extract F_π, the strength of the weak parity-nonconserving (PNC) pion-exchange nucleon-nucleon interaction [31, 34]. Requiring a β-γ coincidence clearly shows that the 1081 keV γ ray is correlated with the β activity recorded in SCEPTAR. The region around the 1701 keV γ ray is shown in Fig. 2(c). With the exception of the 511 keV produced from all positron decays, no evidence for any additional beam contaminants was found in the γ-ray spectra.

Relative γ-ray intensities and β-decay branching ratios were deduced from the fitted peak areas of the γ-ray singles spectrum of Fig. 2(a) and the relative detection efficiencies of the 8π spectrometer that were obtained using standard γ-ray calibration sources of ^{56}Co, ^{133}Ba, and ^{152}Eu. Results from the present work are compared to previous experiments in Tables II and III for the relative γ-ray intensities and decay branching ratios, respec-

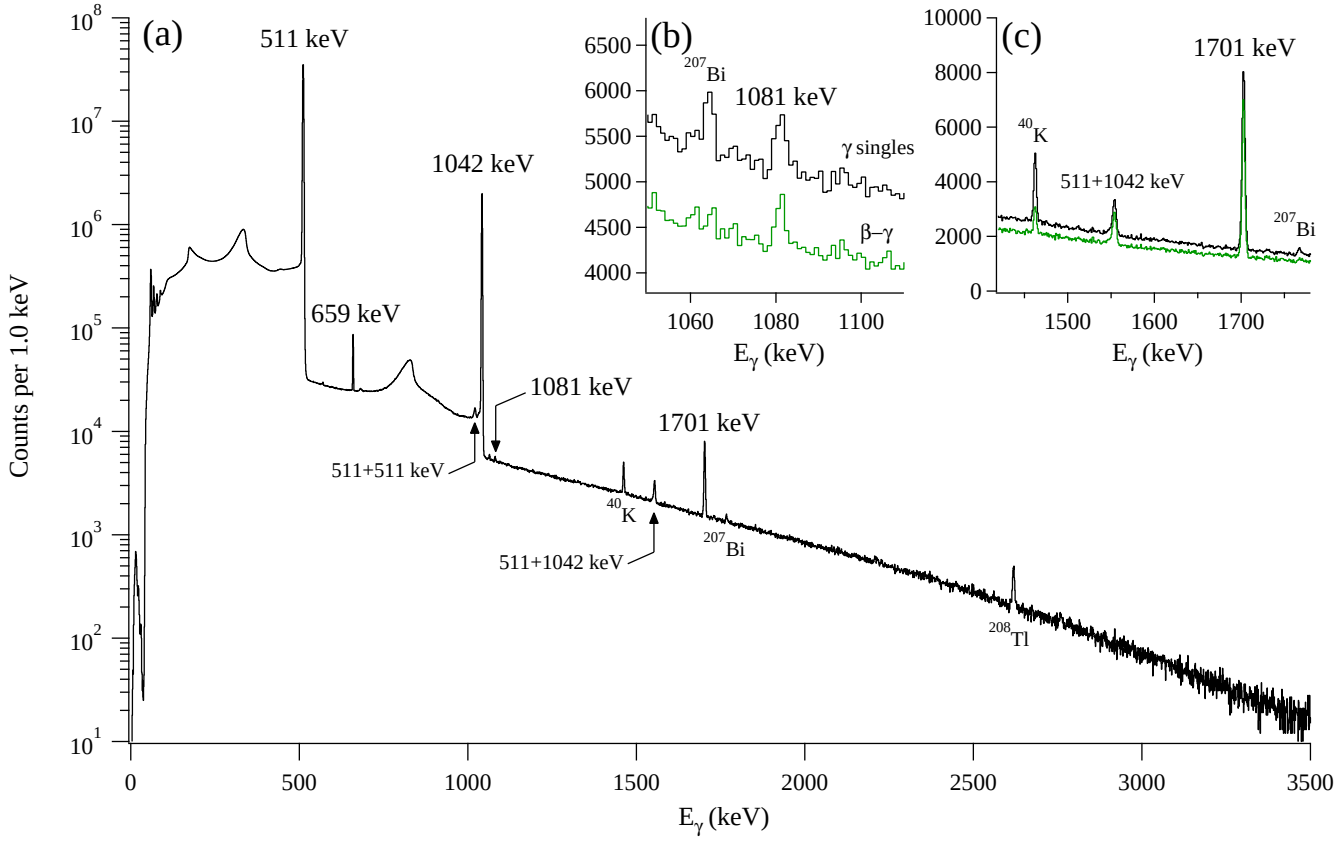

FIG. 2: (Color online) (a) Singles γ-ray spectrum for ^{18}Ne decay for all data collected with amplifier shaping times of 2.0 μs. A time gate was applied that includes the duration of the beam on time (2 min, 5 s, or 2.5 s) plus 15 s (9 halflives of ^{18}Ne) after the beam was turned off. Natural room background lines are indicated. A total of 6×10^6 counts were obtained in the 1042 keV photopeak. In (b) and (c) the β-γ coincidence spectrum is also shown (with an arbitrary normalization factor) to highlight the weak first-forbidden 0^+ to 0^- decay branch to the 1081 keV state and the high-energy region near 1701 keV, respectively.

tively. In general there is very good agreement between our results and those of previous studies. The improved precision in the relative intensity of the 659 keV γ-ray transition will improve the correction for γ-ray feeding into the 1042 keV level in the evaluation of the absolute superallowed branching-ratio [1]. The calculation of the branching ratio to the 1081 keV level includes the possibility that this state could, in principle, be fed by a 620 keV γ ray originating from the 1701 keV level above (see Fig. 1). In previous studies of ^{18}Ne decay [32, 33], the value of $(0.1 \pm 0.1)\%$ was adopted for the γ-ray branching ratio for this possible 620 keV transition from the upper limit of $< 0.2\%$ previously established in nucleon-transfer reaction studies [35]. Using the present data, a more stringent upper limit of $< 0.12\%$ at 90% confidence was established for this transitions from the analysis of the background-subtracted γ-γ coincidence spectrum gated on the 1081 keV γ ray. This corresponds to a relative intensity of $< 0.003\%$ with respect to the 1042 keV γ ray as shown in Table II. In the calculations of the branching ratios for the present work (Table III), we have therefore adopted the value $(0.06 \pm 0.06)\%$ for this possible γ-ray feeding into the 1081 keV level.

B. Beam composition and purity

In the first ^{18}Ne experiment, contamination from ^{17}F was observed in the $A = 18$ mass-separated beam with an average intensity of 2.1×10^4 ions/s. This isotope ($T_{1/2} = 64.5$ s [36]) was produced in the target and transported from the ECR ion source as a singly-ionized HF molecule. While neither ^{17}F nor ^{18}F positron decays give rise to any characteristic γ rays, their relative amounts can be determined from the time-dependent activity of the 511 keV γ-ray that follows positron annihilation. A typical activity curve for 511 keV-gated γ-ray singles events is shown in Fig.3(a) for an individual run consisting of 24 cycles ($\sim$1 hour of data collection). These data were dead-time and pile-up corrected according to the methods described below.

Fits to the grown-in and decay activity were used to deduce the individual contributions of each beam constituent to the total measured activity curve and determine the overall beam composition and purity. Beam intensities were treated as free parameters while beam-on and beam-off times and the half-lives of each isotope (^{17}F, ^{18}F, and ^{18}Ne) were fixed at their nominal values.

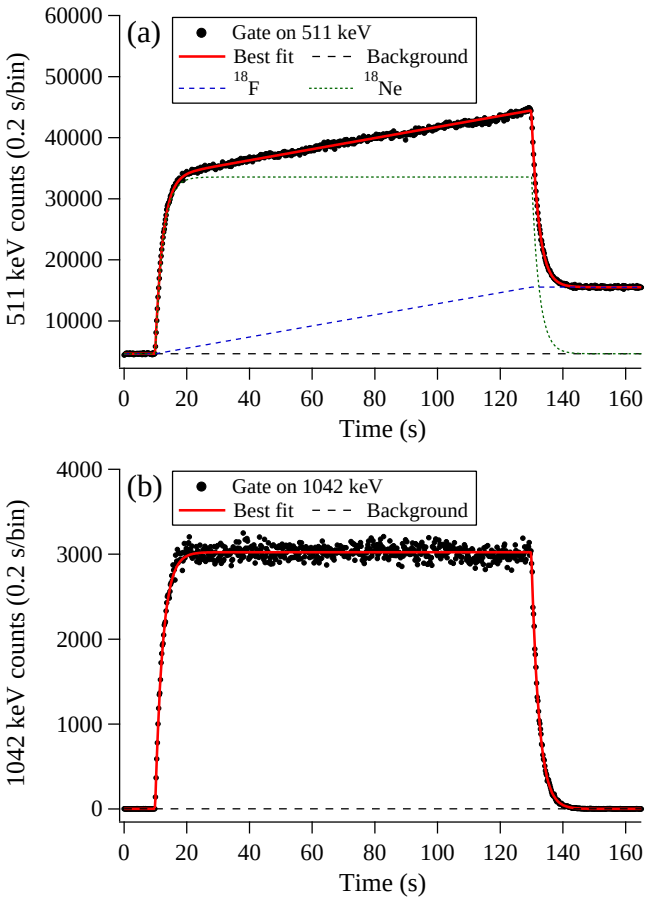

FIG. 3: (Color online) (a) Activity curve for 511 keV γ-ray gated events with corrections for dead time and pulse pile up applied. The contributions to the best-fit activity curve are shown for ^{18}F, ^{18}Ne, and an overall constant background. The ^{18}F activity curve includes contributions from both ions delivered in the beam and those produced following the decay of implanted ^{18}Ne ions. (b) Activity curve for 1042 keV γ-ray gated events that arise exclusively from the decay of ^{18}Ne.

The additional ^{18}F daughter activity arising from the decay of implanted ^{18}Ne ions was also included in the fit. This contribution does not require any additional free parameters as it is directly obtained from the ^{18}Ne activity. An overall constant background was also included with its value constrained using the 10 s of data collection before the beam was turned on.

The best overall fit to the 511 keV-gated γ-ray activity curve is consistent with there being no ^{17}F beam contamination. The individual contributions from ^{18}Ne and ^{18}F to the total measured activity obtained from a two-component fit (with the ^{17}F beam intensity fixed to 0) are overlayed for comparison in Fig. 3(a). From this analysis, the beam intensities of ^{18}Ne and ^{18}F were deduced to be 8.5×10^5 ions/s and 2.5×10^7 ions/s, respectively. Addition of a third component to the fit function, with the ^{17}F half-life fixed at its nominal value and its intensity treated as a free parameter, yielded a non-physical (negative) value of $(-1.1 \pm 0.5)\times10^4$ ions/s. This result was used to set an upper limit on the ^{17}F beam intensity at $< 3.8\times10^3$ ions/s with 90% confidence. Compared to the first experiment with the ECR, production of H^{17}F molecules with the FEBIAD ion source was suppressed by at least an order of magnitude relative to ^{18}Ne (see Table I). The higher plasma temperature in the FEBIAD appears to be sufficient to dissociate HF molecules or prevent their formation. Beam intensities from both experiments are compared in Table I.

TABLE IV: Initial activities R and sample purities p for the $A = 18$ beam constituents ^{18}Ne, ^{18}F, and ^{17}F following implantation times of either 5 s or 120 s. Values were calculated from the beam intensities provided in Table I and the half-lives of the particular isotopes. No evidence for ^{17}F molecular contamination was observed from the FEBIAD source and quoted values represent upper limits at 90% confidence.

Isotope Species	R_{120} (decays/s)	p_{120} (%)	R_5 (decays/s)	p_5 (%)
^{18}Ne	8.5×10^5	72.7	7.4×10^5	98.22
^{18}F	3.2×10^5	27.0	1.3×10^4	1.75
^{17}F	$<2.8\times10^3$	<0.24	$<2.0\times10^2$	<0.03

Although significant amounts of ^{18}F were present in the beam and created from the decay of ^{18}Ne, its long half-life ensured that the unwanted β and 511 keV γ-ray activities produced from their decays were relatively small compared to the ^{18}Ne activity. Assuming beam implantation times of either 5 s or 120 s that are relevant to the present work, the individual contributions of each of these species to the total activity is shown in Table IV. With a beam-on time of only 5 s for example, 98.2% of the total activity is from ^{18}Ne decay.

The sample purity of the activity can be greatly improved by selecting γ rays that uniquely follow the decay of the isotope(s) of interest. The activity spectrum for the 1042 keV γ-rays that follow $\sim$8% of all ^{18}Ne decays is shown in Fig. 3(b). It should be emphasized that both spectra in Fig. 3 were obtained from the same data. The only difference is the γ-ray gate that has been applied. This degree of selectivity to achieve high-purity decay activity curves is one of the main motivations for using delayed γ rays to determine β decay half-lives with high precision and motivated the need for a technique, which has now been developed, to accurately correct for pile-up losses associated with γ-ray detection [25]. Small and time-dependent backgrounds underneath the 1042 keV photopeak could, in principle, arise due to Compton scattering from higher energy γ-rays and inner-bremsstrahlung produced from electron-capture processes. For the only measured contaminant, ^{18}F, all of these processes are energetically forbidden given that the electron-capture Q value is only 1655 keV [21]. While these processes would be energetically allowed for the case of ^{17}F, the activity from the decay of this isotope was already undetectable in the

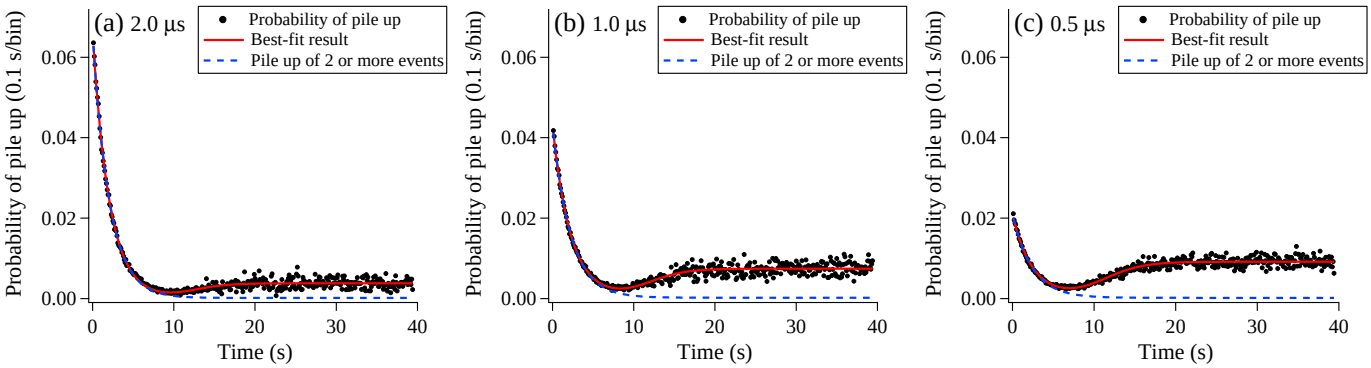

FIG. 4: (Color online) Typical pile-up probability curves and resulting best fits for single runs with amplifier shaping times of (a) 2.0 μs, (b) 1.0 μs, and (c) 0.5 μs. The dashed lines are the corrections applied to the γ-ray gated data. See text for details.

511 keV γ-ray gated data obtained from long implantation times. Employing short beam-on times and gating on 1042 keV γ rays would imply that this possibility can be safely neglected. A fit to the 1042 keV γ-ray gated activity spectrum of Fig. 3(b) that considered only ^{18}Ne decay and a constant background provides an excellent overall description of these data. The half-life deduced from this fit, $T_{1/2} = 1.670(9)$ s, is also in good agreement with the average ^{18}Ne half-life $T_{1/2} = 1.6670(19)$ s [1]. We therefore conclude that the 1042 keV γ-ray energy gate can be used to provide ^{18}Ne decay-activity curves with negligible time-dependent contributions from the decays of the measured in-beam contaminants in the present experiment.

III. HALF-LIFE MEASUREMENT

In the first experiment, the half-life of ^{18}Ne was deduced from a total of 4254 implantation-and-decay cycles with an average beam intensity of $\sim 4\times10^5$ ions/s. The overall precision obtained in the resulting half-life, $T_{1/2} = 1.6656(19)$ s, was entirely limited by the $\pm$ 0.0017 s statistical uncertainty [23]. A small systematic uncertainty of $\pm$ 0.0009 s was added in quadrature that was estimated from the variation of the half-lives obtained at each individual amplifier shaping-time setting and the estimated systematic uncertainty of 4% of the pile-up correction that has been conservatively assigned to the correction method itself [25]. In the second experiment, an additional 3192 decay cycles were obtained over 54 experimental runs using the higher-intensity ^{18}Ne beam provided by the FEBIAD ion source. The statistical precision in the half-life for this new data set is $\pm$ 0.0009 s, which is approximately a factor of 2 times more precise. Given that the experimental apparatus and the analysis methods are identical for the two data sets, the systematic uncertainties (if derived independently) cannot be trivially combined at the end. However, since the previous result was limited by statistics rather than systematic effects, the 15 runs from the original data set have been re-analyzed with the 54 runs of the present data set. A systematic uncertainty is then deduced from the combined data set. The improved half-life of ^{18}Ne presented below therefore supersedes, and should not be averaged with, the previously published value in Ref. [23].

Data were collected with cycle times of 5-t_b-40-1 s where the beam-on time was either $t_b = 2.5$ s (16 runs), 5.0 s (38 runs), or 7.0 s (15 runs). The decay time of $t_d = 40$ s, or approximately 24 half-lives of ^{18}Ne, was chosen to be long enough to ensure that the ^{18}Ne activity had sufficient time to decay to a negligible level so that the overall constant background (a free fit parameter) could be adequately constrained. A total of 7446 cycles were collected under several conditions that were varied throughout the two experiments on a run-by-run basis. As described above, amplifier shaping times were varied between 0.5 μs, 1.0 μs, and 2.0 μs and the dead time of the data acquisition was chosen to be "variable" (measured event-by-event using the time stamp of the data acquisition), 27 μs fixed and non-extendible, or 40 μs fixed and non-extendible. Dead-time corrections varied between 10% and 50% at the start of the decay activity.

The half-life was determined by selecting events in which the 1042 keV photopeak was detected in any of the 20 HPGe detectors of the 8π spectrometer. After applying detector energy calibrations, the widths of the γ-ray energy gates used in the analysis were common for every detector at a particular amplifier shaping time. Energy gates were chosen to include the entire photopeak plus one channel of background on either side. This corresponded to gate widths of 14, 18, and 26 keV for the 2.0 μs, 1.0 μs, and 0.5 μs shaping times, respectively. For each run, a minimum threshold was applied to the number of 1042 keV counts collected in each cycle in order to remove those cycles where the beam delivery was interrupted. The final cycle in every run was also rejected from the analysis as the acquisition was often stopped before it was completed. These selection criteria removed a total of 294 cycles, or approximately 4% of the 7446 total cycles collected over the course of the two separate experiments.

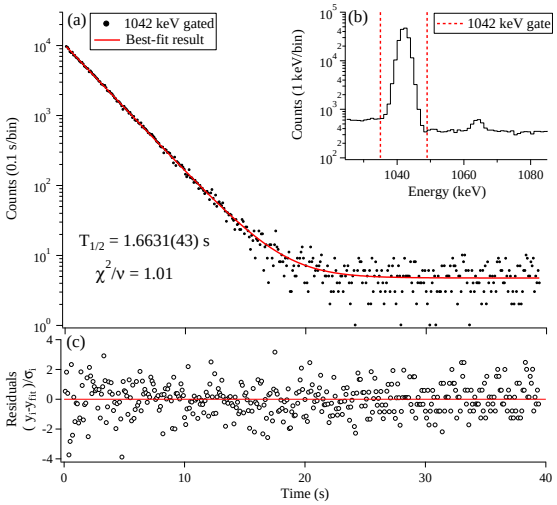

FIG. 5: (Color online) (a) Decay activity for 1042 keV γ-ray photopeak events for a single run consisting of 75 decay cycles. (b) Portion of the γ-ray singles spectrum and the 1042 keV gate (dashed lines) used in the analysis and (c) fit residuals for the decay curve.

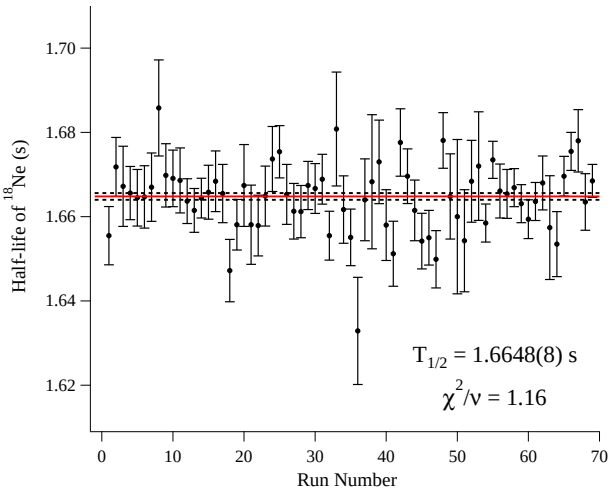

FIG. 6: (Color online) Half-life of ^{18}Ne determined for each of the 69 experimental runs. The average half-life and its statistical uncertainty $T_{1/2} = 1.6648(8)$ s are indicated by the solid and dashed lines, respectively.

Decay data gated on the 1042 keV γ ray were dead-time and pile-up corrected on a event-by-event basis using the procedures described in Ref. [25]. In the high-rate data set, pile-up corrections at the start of the decay activity ranged between approximately 2, 4, or 6% for the amplifier shaping times of 0.5 μs, 1.0 μs, or 2.0 μs, respectively. The pile-up corrections of $\approx$ 6% at the start of the decay activity for the 2 μs shaping times are comparable to the largest corrections that were applied in Ref. [25] and are significantly larger than the corrections required in the previous ^{18}Ne half-life measurement [23]. In Fig. 4, a comparison between sample time-dependent pile-up probability distributions that were used to correct the γ-ray gated decay data on a bin-by-bin basis, are shown for three separate runs collected at the three different shaping times. These distributions were obtained from the time-dependent ratio between *all* piled-up events to the total number of trigger events for each run. No γ-ray gate was applied to these data since, by definition, energy information is lost for true pile-up events. Pile-up probabilities decrease approximately exponentially with a half-life that is very nearly half that of ^{18}Ne ($\sim$0.8 s) because true pulse pile up requires at least two γ rays. In all cases, a minimum appears around 8 s and arises from a low rate of saturating events (cosmic rays) that have a very high probability for individually triggering the pile-up circuitry of the amplifiers. These events dominate the shape of the pile-up probability distributions at late times where the probability for two-or-more γ ray pile-up events in the background is extremely low. With longer shaping times, the probability for true pulse pile-up of two-or-more events is larger and thus the minima are suppressed with increasing shaping time. In the half-life analysis, this cosmic-ray contribution must be subtracted from the total fit to obtain the time-dependent pile-up corrections (dashed lines in Fig. 4) that should be applied to the γ-ray gated decay data, as described in detail in Ref. [25].

Following the corrections for dead-time and pile-up losses, the half-life of ^{18}Ne was determined by fitting the sum of the individual cycles in each run using a maximum likelihood χ^2 minimization routine that has been described previously [37, 38]. The fit function considered only the exponential decay of ^{18}Ne as additional sources of time-dependent decay activity in the 1042 keV γ-ray energy gate were concluded to be negligible from the discussion above in Sec. II B. The fit function included free parameters for the initial activity of ^{18}Ne, its half-life, and an overall constant background. A sample decay curve from 1042 keV γ-ray gated events that consists of 75 cycles is shown in Fig. 5(a) with the corresponding best-fit and reduced χ^2 value. The relevant portion of the γ-ray spectrum with the γ-ray energy gate that was applied in the analysis is shown in Fig. 5(b). The bin-by-bin fit residuals are provided in Fig. 5(c). The statistical precision achieved from an individual run was approximately $\pm$ 0.25%.

The half-lives of ^{18}Ne deduced from each of the 69 experimental runs that were collected over the 2 experiments are presented in Fig. 6. Treating each run as independent measurements, the average half-life and its statistical uncertainty is $T_{1/2} = 1.6648(8)$ s, with a reduced χ^2 value of 1.16. This result is a factor of two times more precise than, and in excellent agreement with, the previous value $T_{1/2} = 1.6656(17)$ s obtained from only the first experiment (the first 15 runs in Fig. 6), as reported in Ref. [23].

A. Systematic Uncertainties

Searches for possible sources of rate-dependent systematic effects that could bias the high-precision half-life determination included a leading-channel removal analysis where the half-life of ^{18}Ne is deduced as decay data collected at the highest rates are incrementally removed. This analysis is presented in Fig. 7 for the entire data set when the pile-up correction has been applied to the data (closed circles) and when it has been neglected (open circles). Each data point represents the half-life of ^{18}Ne obtained from the weighted average of the entire 69 runs when data are removed from the start of the decay activity curve for each run in steps of 5 channels (0.5 s) up to a total of 50 channels (5.0 s) or 3 half-lives of ^{18}Ne. When the pile-up corrections are not included, there is a clear correlation between the deduced half-life and the counting rate that is absent once the pile-up corrections have been applied to the data. After removing the first $\sim$ 3.5 s (2 half-lives of ^{18}Ne) the corrected and uncorrected half-life values agree, indicating that counting rates are sufficiently low at this time that the pile-up corrections are negligible. At the start of the decay activity, the ^{18}Ne half-life was deduced to be $T_{1/2}$ = 1.6648(8) s from the data with the pile-up correction applied and $T_{1/2}$ = 1.6765(8) s from the uncorrected data. In terms of the half-life, the total correction for detector pulse pile-up is therefore $\sim$0.7%, or nearly 15 statistical standard deviations. The longer half-life obtained in the uncorrected analysis is consistent with the fact that 1042 keV γ-ray photopeak events are more likely to be piled-up and thus lost from the analysis at high counting rate.

In radioactive beam experiments with noble-gas ions, time-dependent diffusion of a particular fraction of the implanted sample from the collector material can be a significant concern [39–41]. The above channel-removal analysis indicates that any rapid release of significant quantities of the implanted ^{18}Ne ions is negligible compared with the level of statistical precision obtained in the experiment. The possibility of diffusion on longer time scales was studied in the previous work by comparing the deduced half-life of the longer-lived ^{23}Ne isotope ($T_{1/2}$ = 37 s) to a previous measurement performed by trapping ^{23}Ne atoms in the gas phase [42]. The excellent agreement between these two results demonstrated that diffusion on longer time scales can similarly be neglected in the analysis of ^{18}Ne ions with our experimental apparatus. In addition, a high-precision ^{19}Ne half-life measurement was performed using the same experimental setup and the result, $T_{1/2}$ = 17.262(7) s [43], has been confirmed at the level of $\pm$ 0.04% by an independent measurement recently performed at GANIL [44]. Given these considerations, we conclude that any diffusion of implanted ^{18}Ne ions in the present experiment is negligible in comparison to the $\pm$ 0.05% statistical precision of our measurement.

During the course of the experiment, several modifications to the electronics settings were made on a run-by-run basis to ascertain whether or not additional sources of systematic uncertainty could arise from the electronics modules themselves or by the correction and analysis procedures that were applied to the data. Amplifier shaping times were adjusted between 0.5 μs, 1.0 μs, and 2.0 μs and, as described above, this modifies the probability for pile up and hence the magnitude of the resulting pile-up corrections (see Fig.4). Acquisition dead times were also adjusted on a run-by-run basis. The average ^{18}Ne half-lives obtained for each particular group of runs collected under each of these electronics settings were calculated and the results are shown in Fig.8. As every run can only have a single shaping-time or dead-time, the average half-life of each group is equivalent to $T_{1/2}$ = 1.6648(8) s, the weighted average of the entire data set. A third group is also shown in Fig. 8 that calculates the average ^{18}Ne half-life from the previous experiment $T_{1/2}$ = 1.6656(17) s and compares it to the result, $T_{1/2}$ = 1.6646(9) s, obtained from the new data added in the second experiment.

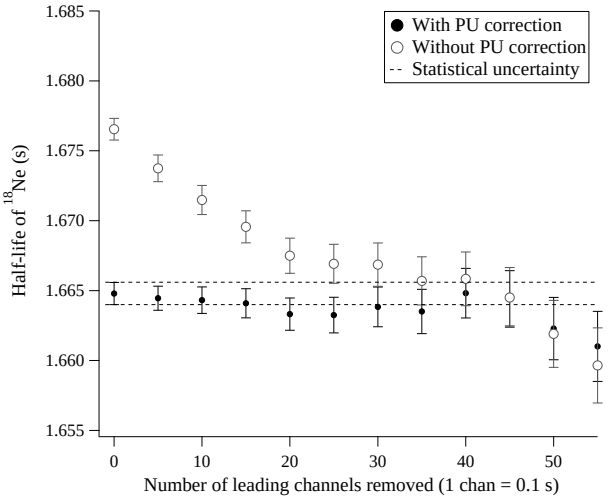

FIG. 7: Half-life of ^{18}Ne versus the number of leading channels removed (1 channel = 0.1 s). The deduced half-life is compared with and without the corrections applied for detector pulse pile up out to 5.0 s or 3 half lives of ^{18}Ne. The statistical uncertainty ($\pm$ 1σ) of the pile-up corrected half-life when no channels have been removed is overlayed for comparison.

To estimate a systematic uncertainty from these comparisons, reduced χ^2 values were calculated on a run-by-run basis in Fig. 6, and for each group of adjustable electronic settings as indicated in Fig. 8. The largest reduced χ^2 value was 1.68 and was obtained from the ^{18}Ne half-lives grouped according to the dead-time setting. Following the method of the Particle Data Group [45], the square root of this value is used to increase the statistical uncertainty in order to account for any remaining and unidentified systematic effects. Assuming that the total uncertainty of $\pm$ 0.0010 s obtained from this procedure can be expressed as the quadrature sum of the statistical and systematic uncertainties, the value of $\pm$ 0.0007 s is obtained for the systematic uncertainty, which is nearly

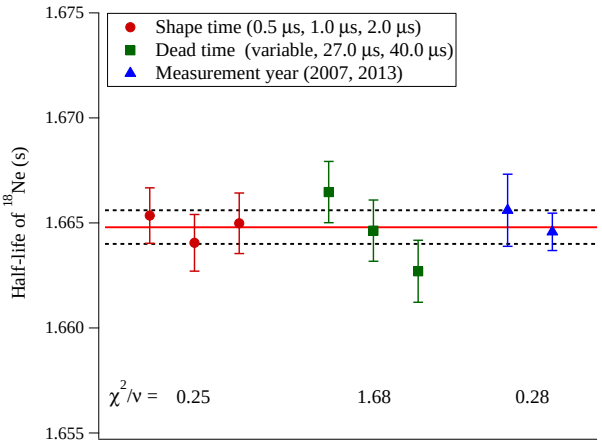

FIG. 8: (Color online) Half-life of ^{18}Ne grouped according to adjustable electronic setting. The reduced χ^2 values for each of the three settings are indicated.

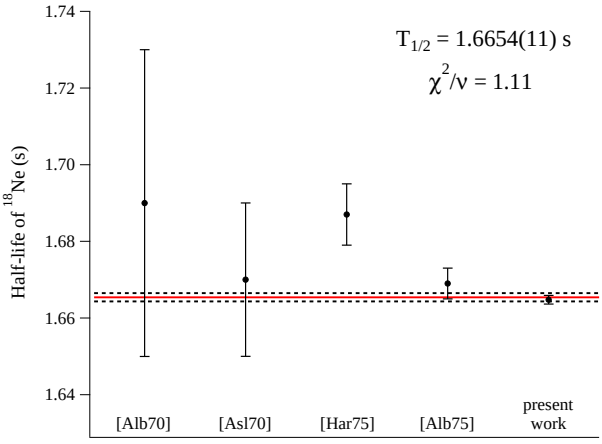

FIG. 9: (Color online) Summary of ^{18}Ne half-life measurements and comparison to the present work. References to previous measurements are Alb70 [46], Asl70 [47], Har75 [24], and Alb75 [48], respectively. The world average ^{18}Ne half-life obtained from these data and the averaging procedure described in Ref. [1] is $T_{1/2} = 1.6654(11)$ s.

equivalent to the ± 0.0008 s statistical precision. An additional source of systematic uncertainty arising from the application of the pile-up correction procedures described here has been conservatively estimated to be 4% of the total correction itself as described in Ref. [25]. From the 0.0117 s difference between the half-lives obtained with and without the pile-up corrections applied, this additional systematic uncertainty is ± 0.0005 s.

The half-life of ^{18}Ne deduced in the present work can be written as $T_{1/2} = 1.6648(8)(7)(5)$ s, where the first uncertainty is statistical, the second is systematic and was estimated from the variation of the deduced half-lives grouped by the dead-time setting of the data-acquisition system, and the third is a systematic uncertainty associated with the pile-up correction methodology. Combining these uncertainties in quadrature gives the final result, $T_{1/2} = 1.6648(11)$ s, for the half-life of ^{18}Ne. This is approximately a factor of two times more precise than the value previously reported from the first experiment [23]. Our new value replaces the previous one as the data from this first experiment have been included in the present evaluation. The half-life of ^{18}Ne is also in agreement with $T_{1/2} = 1.669(4)$ s [48], the most precise measurement prior to our own, although it is nearly 4 times less precise. A summary of all previous ^{18}Ne half-life measurements is presented in Fig. 9. According to the procedures adopted in Ref. [1] for combining these results, the world-average ^{18}Ne half-life is $T_{1/2} = 1.6654(11)$ s. The evaluation of the uncertainty on the average includes a scale factor of 1.05 (see Ref. [1]) obtained from the square root of the reduced χ^2 value of 1.11 for these data. With an overall precision of ± 0.07 %, which is dominated by the half-life measurement presented in this work, the half-life of ^{18}Ne has now been determined at a level that is expected to be at least ∼3 times more precise than is likely feasible for a high-precision branching-ratio measurement of this superallowed Fermi transition. The ^{18}Ne half-life is therefore not expected to be a limiting factor in establishing a high-precision ft value for the superallowed decay of ^{18}Ne in the foreseeable future.

IV. SUMMARY AND CONCLUSION

High-resolution β delayed γ-ray spectroscopy has been performed following the decay of ^{18}Ne ions implanted at the center of the 8π γ-ray spectrometer at TRIUMF's ISAC facility. The half-life of ^{18}Ne has been determined to be $T_{1/2} = 1.6648(11)$ s following the application of a 0.7% correction that was required to account for systematic and rate-dependent losses associated with detector pulse pile up. This result is approximately a factor of two times more precise than, and in excellent agreement with, our previous measurement that was performed with a prototype ECR ion source. Improved precision on the relative β-decay branching ratios and delayed γ-ray intensities were also obtained and are in very good agreement with previous measurements. These results will provide important input towards future experiments that aim to improve the precision of the ^{18}Ne ft value to the level of ± 0.2% that has now been achieved in two other $T_z = -1$ cases. The case of ^{18}Ne is particularly attractive as it potentially provides a means to discriminate between several theoretical models of isospin symmetry breaking and can be used to investigate the role of nuclear deformation in the calculation of these corrections.

Acknowledgments

We would like to thank the ISAC ion-source and beam development group for their hard work and dedication to the production of the high-quality ^{18}Ne beam necessary for this experiment. This work was partially supported by the Natural Sciences and Engineering Research Council of Canada and the National Science Foundation under Grant No. PHY-0606007. TRIUMF receives federal funding via a contribution agreement through the National Research Council of Canada.

[1] J. C. Hardy and I. S. Towner, Phys. Rev. C **79**, 055502 (2009).
[2] I. S. Towner and J. C. Hardy, Phys. Rev. C **77**, 025501 (2008).
[3] N. Auerbach, Phys. Rev. C **79**, 035502 (2009).
[4] H. Liang, N. V. Giai, and J. Meng, Phys. Rev. C **79**, 064316 (2009).
[5] A. E. Çalik, M. Gerçeklioğlu, and D.I.Salamov, Z. Naturforsch. **64a**, 865 (2009).
[6] W. Satuła, J. Dobaczewski, W. Nazarewicz, and M. Rafalski, Phys. Rev. Lett. **106**, 132502 (2011).
[7] W. Satuła, J. Dobaczewski, W. Nazarewicz, and M. Rafalski, Phys. Rev. C **86**, 054316 (2012).
[8] G. F. Grinyer, C. E. Svensson, and B. A. Brown, Nucl. Instrum. Meth. Phys. Res. A **622**, 236 (2010).
[9] G. C. Ball *et al.*, Phys. Rev. Lett. **86**, 1454 (2001).
[10] A. Piechaczek *et al.*, Phys. Rev. C **67**, 051305(R) (2003).
[11] B. Hyland *et al.*, Phys. Rev. Lett. **97**, 102501 (2006).
[12] G. F. Grinyer *et al.*, Phys. Rev. C **77**, 015501 (2008).
[13] P. Finlay *et al.*, Phys. Rev. C **78**, 025502 (2008).
[14] P. Finlay *et al.*, Phys. Rev. Lett. **106**, 032501 (2011).
[15] G. Melconian *et al.*, Phys. Rev. Lett. **85**, 025501 (2012).
[16] R. G. Helmer, J. C. Hardy, V. E. Iacob, M. Sanchez-Vega, R. G. Neilson, and J. Nelson, Nucl. Instrum. Meth. Phys. Res. A **511**, 360 (2003).
[17] J. C. Hardy *et al.*, Phys. Rev. Lett. **91**, 082501 (2003).
[18] J. C. Hardy and I. S. Towner, J. Phys.: Conf. Ser. **387**, 012006 (2012).
[19] I. S. Towner and J. C. Hardy, Phys. Rev. C **66**, 035501 (2002).
[20] K. Blaum *et al.*, Nucl. Phys. **A746**, 305 (2004).
[21] D. R. Tilley, H. R. Weller, C. M. Cheves, and R. M. Chasteler, Nucl. Phys. **A595**, 1 (1995).
[22] G. Audi, A. H. Wapstra, and C. Thibault, Nucl. Phys. **A729**, 337 (2003).
[23] G. F. Grinyer *et al.*, Phys. Rev. C **76**, 025503 (2007).
[24] J. C. Hardy, H. Schmeing, J. S. Geiger, and R. L. Graham, Nucl. Phys. **A246**, 61 (1975).
[25] G. F. Grinyer *et al.*, Nucl. Instrum. Meth. Phys. Res. A **579**, 1005 (2007).
[26] P. Bricault *et al.*, Rev. Sci. Instrum. **83**, 02A914 (2012).
[27] J. Han *et al.*, Appl. Rad. Isot. **70**, 2581 (2012).
[28] G. C. Ball *et al.*, J. Phys. G **31**, S1491 (2005).
[29] C. E. Svensson *et al.*, Nucl. Instrum. Meth. Phys. Res. B **204**, 660 (2003).
[30] P. E. Garrett *et al.*, Nucl. Instrum. Meth. Phys. Res. B **261**, 01084 (2007).
[31] E. G. Adelberger, C. D. Hoyle, H. E. Swanson, and R. D. V. Lintig, Phys. Rev. Lett. **46**, 695 (1981).
[32] A. M. Hernandez and W. W. Daehnick, Phys. Rev. C **25**, 2957 (1982).
[33] E. G. Adelberger, M. M. Hindi, C. D. Hoyle, H. E. Swanson, R. D. V. Lintig, and W. C. Haxton, Phys. Rev. C **27**, 2833 (1983).
[34] W. C. Haxton, Phys. Rev. Lett. **46**, 698 (1981).
[35] C. Rolfs, H. P. Trautvetter, R. E. Azuma, and A. E. Litherland, Nucl. Phys. **A199**, 289 (1973).
[36] D. R. Tilley, H. R. Weller, and C. M. Cheves, Nucl. Phys. **A565**, 1 (1993).
[37] G. F. Grinyer *et al.*, Phys. Rev. C **71**, 044309 (2005).
[38] V. T. Koslowsky *et al.*, Nucl. Instrum. Meth. Phys. Res. A **401**, 289 (1997).
[39] U. C. Bergmann *et al.*, Nucl. Phys. **A714**, 21 (2003).
[40] V. E. Iacob *et al.*, Phys. Rev. C **74**, 055502 (2006).
[41] A. Knecht *et al.*, Phys. Rev. Lett. **108**, 122502 (2012).
[42] D. E. Alburger, Phys. Rev. C **9**, 991 (1974).
[43] S. Triambak *et al.*, Phys. Rev. Lett. **109**, 042301 (2012).
[44] P. Ujić *et al.*, Phys. Rev. Lett. **110**, 032501 (2013).
[45] J. Beringer *et al.*, Phys. Rev. D **86**, 010001 (2012).
[46] D. E. Alburger and D. H. Wilkinson, Phys. Lett. **B32**, 190 (1970).
[47] E. Aslanides, F. Jundt, and A. Gallmann, Nucl. Phys. **A152**, 251 (1970).
[48] D. E. Alburger and F. P. Calaprice, Phys. Rev. C **12**, 1690 (1975).